 doi:10.20944/preprints202110.0448.v2

Article

Pseudo-static simplified analysis method of the pile-liquefiable soil interaction considering rate-dependent characteristics

Xinlei Zhang [1], Zhanpeng Ji [1], Hongmei Gao [1,*], Zhihua Wang [1,*], and Wenwen Li [2,]

[1] Research Center of Urban Underground Space, Nanjing Tech University, Nanjing 211816, China; xinlei.zhang@njtech.edu.cn (X.Z.); zhanpeng18@njtech.edu.cn (Z.J.)
[2] Business school, Changshu Institute of Technology, Suzhou 215500, China; lwwgeo@hotmail.com (W.L.)
* Correspondence: hongmei54@njtech.edu.cn (H.G.); wzh@njtech.edu.cn (Z.W.)

Abstract: The lateral pressure generated by liquefied soil on pile is a critical parameter in the analysis of soil-pile interaction in liquefaction-susceptible sites. Previous studies have shown that liquefied sand behaves like a non-Newton fluid, and its effect on piles has rate-dependent properties. In this study, a simplified pseudo-static method for liquefiable soil-pile interaction analysis is proposed by treating the liquefied soil as a thixotropic fluid, which considers the rate-dependent behavior. The viscous shear force generated by the relative movement between the viscous fluid (whose viscosity coefficient varies with excess pore pressure and shear strain rate) and the pile was assumed to be the lateral load on the pile. The results from the simplified analysis show that the distribution of bending moment is in good agreement with experiments data. Besides, the effects of various parameters, including relative density, thickness ratio of non-liquefiable layer to liquefiable layer, and frequency of input ground motion, on the pile-soil rate-dependent interaction were discussed in detail.
This manuscript has been preprinted on October 29, 2021, at the website for https://www.preprints.org/manuscript/202110.0448/v1.

Keywords: soil liquefaction; pile-soil interaction; rate-dependent; simply analysis; influence factors analysis

1. Introduction

Pile foundation has been the preferred foundation form for structure founded in the liquefiable field [1]. However, the failures of pile foundations caused by saturated sand liquefaction were observed in many earthquakes around the world (e.g., Alaska earthquake (1964) [2], Niigata earthquake (1964), Edgecumbe earthquake (1987) [2], Indonesia earthquake (2018) [2], Wenchuan earthquake (2008) [3], Tohoku earthquake (2011) [4], etc.). Accordingly, the performance of pile foundations during liquefaction remains an area of active research [5–7].

The soil-structure interaction is a complicated and pseudo-statically procedure driven by the lateral displacement of the field [8]. The soil-pile interaction in liquefiable sand is significantly affected by relative density, strength degradation, excess pore pressure, prior displacement history, and loading rate [9]. However, the mechanical mechanism of liquefied soil-pile interaction is still uncertain, and it's difficult to quantify and evaluate the influence of various factors on the soil-pile interaction.

In general, the studies on seismic performance of pile-soil system are carried out by the following methods: model or in-situ test [6,10–12], simplified analysis methods (such as *p-y* curve, p is the force soil acts on the unit length of pile, y is the lateral displacement), finite element [13–15] and theoretical analysis [7,16]. In practice, the shake table test and in-situ test have disadvantages such as high cost and long time-consuming. The application of finite element numerical analysis method in engineering practice is limited due to the difficulty of modeling, low calculation efficiency and difficult parameter

Preprints (www.preprints.org) | NOT PEER-REVIEWED | Posted: 28 March 2022 doi:10.20944/preprints202110.0448.v2

calibration. The simplified calculation method is usually preferred in practice due to the advantages of simplicity, high efficiency, and easy engineering implementation [17]. The *p-y* curve method based on Winkler foundation beam assumption is widely applied to model pile-soil laterally interaction, whereby the soil-structure interaction is modeled employing *p-y* curves as shown in **Figure 1** [18]. At present, the simplified models based on *p-y* curve method include Penzien model [19], Novak model [20], Nogami model [21], Naggar model [22] and Boulanger model [23].

The majority of simplified methods for pile-soil interaction, regard liquefied soil as solid, which is contradictory to the definition of liquefaction by the American Society of Civil Engineers, that is, the process of soil transforms from solid to liquid. These methods considered the pile-soil interaction as the relationship between lateral load on the pile and soil deformation. Moreover, the influence of liquefaction on pile-soil interaction was considered using the strength attenuation method [18], such as adjusting soil spring stiffness, modifying *p-y* curve (i.e., residual strength method [24], zero strength method [25], *p*-multiplier(α) and C_u-factor [26]) or recalculating soil modulus according to effective stress. The *p-y* curve method is well used in the analysis of pile-soil interaction in non-liquefied foundations; however, it is not completely suitable for pile-soil interaction analysis in liquefied soil without the reliable *p-y* curves for liquefied soils [27]. Therefore, the appropriate description of the lateral pressure of liquefaction soil on piles is a key problem in pile-soil interaction simplified analysis.

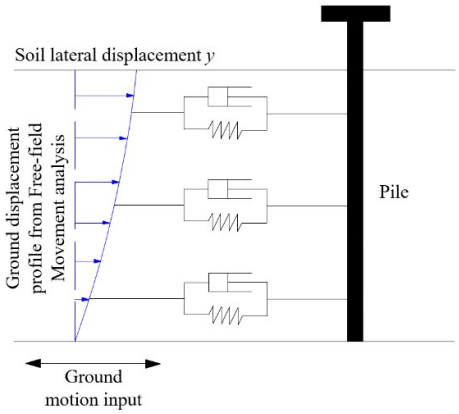

Figure 1. Schematic diagram of *p-y* curve method.

Proper assessment of the characteristics of liquefied soil is necessary for the analysis of the liquefiable soil-pile interaction. Various studies have shown that the liquefied soil behaves like fluid [3,28–33] and exhibits rate-dependent characteristics [13,34,35] which are caused by viscous nature [35]. Wang. et al [36] considered the soil fabric as a fluid net-type structure and presented a unified thixotropic fluid model describing the behavior of the liquefiable soil in response to cyclic loading. However, the previous simple analysis methods of pile-soil interaction only considered the strength reduction of soil, and the fluid characteristics i.e., the rate effect [37] of liquefied sand were ignored. Ignoring the rate-dependent effect in the analysis of liquefiable soil-pile interaction may underestimate the dynamic response of pile foundation, resulting in misjudgment of the seismic failure mechanism of pile foundation in the liquefaction field.

In the present study, a simplified analysis method based on the hydrodynamics theory was proposed to investigate the rate-dependent interaction of liquefied soil and pile. In this model, the liquefied soil is treated as a thixotropic fluid and the viscous shear force related to the shear strain rate and apparent viscosity of liquefied soil is applied to replace the conventional soil pressure acting on the pile. Based on these assumptions, the simplified analysis method of pile-soil rate-dependent interaction is described in detail. Then, based on two cases with different soil profiles, the validity of the

 doi:10.20944/preprints202110.0448.v2

simplified analysis method is demonstrated by comparing the results of the simplified analysis method with that of experiments and other methods. Finally, the effects of the relative density of foundation soil, the thickness ratio of crust non-liquefiable layer to liquefiable layer, and the ground motion frequency on the bending moment and lateral displacement of pile are discussed in detail.

2. Principle and Process of Simplified Analysis Method

2.1. The General Process of Simplified Analysis Method

The analytical model proposed in this study is shown in **Figure 2**. It is assumed that the soil is homogeneous and isotropic. The simplified analytical model is composed of two main components: a) a free field system that is not affected by pile to achieve the ground displacement. b) a lumped mass model of the pile. In this method, the liquefied soil is assumed as a liquid and its lateral loading applied on the pile is related to the shear strain rate and apparent viscosity, which is independent of the ground displacement. Whereas the lateral loading of the non-liquefiable soil layer is dependent on the displacement and strength of soil, and the relative displacement is applied to the pile system through soil springs to model the pile-soil interaction in the non-liquefiable soil. The ideas and steps of the pseudo-static simplified analysis method to describe the pile-soil rate-dependent interaction proposed in this study are as follows.

(1) The acquisitions of the response of each soil layer. A one-dimensional free-field response analysis is carried out to obtain shear strain, acceleration, lateral displacement of each soil layer based on soil profile characteristics and a given base acceleration time history. The maximum acceleration and soil displacement along the pile length during shaking can be obtained.

(2) The acquisitions of maximum shear strain rate of the soil. The shear strain rate of liquefiable soil can be obtained by calculating the time derivative of the shear strain time history achieved by step (1).

(3) The calculation of maximum viscous shear stress. The viscous shear stress acting on the pile is calculated according to the thixotropic fluid constitutive model.

(4) The pile is discretized using the concentrated mass model. On one hand, for the liquefiable layers department (without the soil springs in this interval), the per unit length force analysis of pile is carried out to obtain the lateral viscous shear loading of each soil layer acting on the pile. On the other hand, the soil springs are applied to model the pile-soil interaction in the non-liquefiable soil, and then the maximum lateral displacements of free-field as input are imposed on the springs at corresponding depths. The spring coefficients are calculated according to Mindlin's solution [38]. The lateral inertia force is applied to the concentrated mass points.

(5) The bending moment and lateral displacement of pile response are calculated using the static method.

2.2. Thixotropic Fluid Constitutive Model of Liquefiable Soil

Mao et al. [37] found that the liquefied soil acting on the pile behaves like a viscous fluid, and the bending moment of the pile is proportional to soil velocities (i.e., shear strain rate), the lateral force of liquefied soil acting on the pile has rate-dependent characteristics. To present the rate-dependent nature in this simplified analysis method of pile-soil interaction, the thixotropic constitutive model describing the fluid characteristics of saturated sand was established by Wang et al. [36] is used in this study. The influence of excess pore pressure and apparent viscosity representing the deformation resistance of liquefied sand on the flow effect is considered in the thixotropic constitutive model, and the expression of the model is as follows:

Preprints (www.preprints.org) | NOT PEER-REVIEWED | Posted: 28 March 2022 doi:10.20944/preprints202110.0448.v2

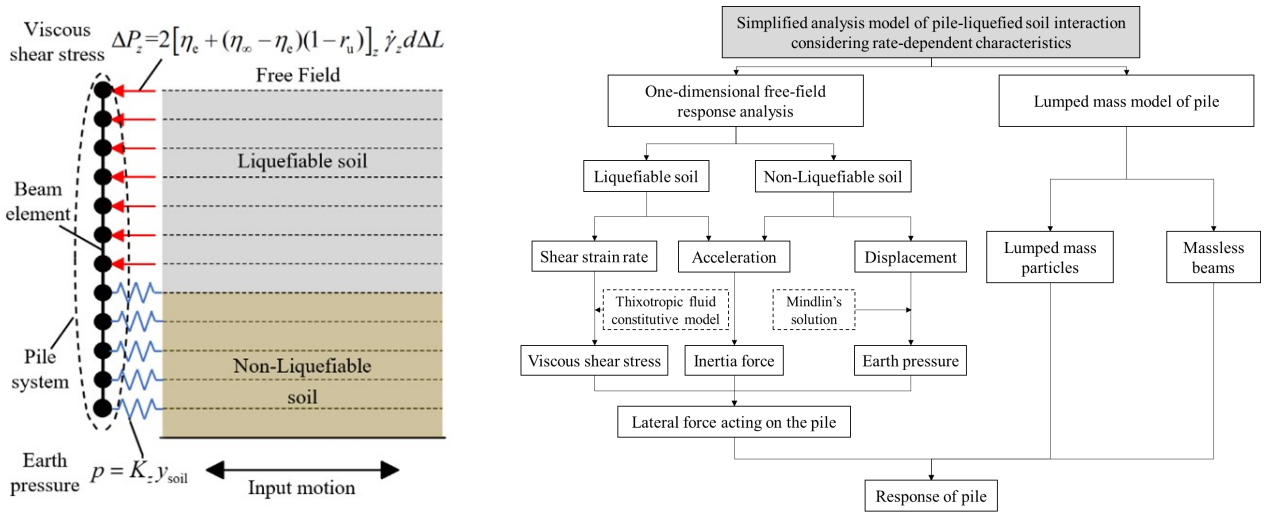

Figure 2. Analytical scheme for the simplified analytical method considering rate-dependent characteristics: (a) Schematic diagram of the pseudostatic method; (b) Chart for the model procedure.

$$\tau=[\eta_e+(\eta_\infty-\eta_e)(1-r_u)]\dot{\gamma} \quad (1)$$

where τ and $\dot{\gamma}$ are the shear stress and shear strain rate of the soil, respectively, r_u is the excess pore pressure ratio, η_e and η_∞ are the viscosity coefficient in the initial equilibrium state ($r_u = 0$) and limit equilibrium state ($r_u = 1$), these two parameters are related to the effective confining pressure and relative density, which can be found in reference [36, 39].

2.3. Seismic Response Analysis of Free-Field

To describe the soil-pile interaction, the dynamic shear strain and lateral displacement response of the soil needs to be obtained. The effect of the pile on soil movement was not considered to simplify the analysis. Therefore, the liquefiable site was regarded as a free site, and its acceleration, displacement, and shear strain dynamic responses can be obtained through one-dimensional equivalent-linear site response analyses. The equivalent-linear site response software, Proshake, which is widely used in the site seismic response analysis, was utilized to generate the dynamic response of soil layer. The variation curve of shear modulus G and damping ratio λ with the shear strain γ expressing the nonlinear characteristics of soil layer, as well as the initial shear modulus (maximum shear modulus G_0), initial damping ratio λ_0 and shear velocity v_s of each soil layer should be given in Proshake software.

Based on the wave theory, the shear wave velocity of soil layer can be calculated by the following formula:

$$v_s=\sqrt{\frac{G_0}{\rho}} \quad (2)$$

where v_s is the shear velocity of soil, ρ is the soil mass density.

As shown in **Figure 3**, the variation curves of G/G_0-γ_a, λ-γ_a recommended by Seed and Idriss [40,41] were adopted in this study. In addition, the initial shear modulus G_0 of each soil layer needs to be determined in one-dimensional equivalent linear analysis. The value of G_0 can be decided in two methods, one is the empirical formula established by the laboratory test, and the other is to use the field shear wave velocity test results. In this study, the empirical formula of the maximum dynamic shear modulus G_0 of sand proposed by Seed and Idriss (1970) [40] is adopted:

Preprints (www.preprints.org) | NOT PEER-REVIEWED | Posted: 28 March 2022 doi:10.20944/preprints202110.0448.v2

$$G_0=21.7K_{\max}P_a\left(\frac{\sigma_c^{'}}{P_a}\right)^{0.5} \quad (3)$$

where K_{max} is a parameter determined by the relative density D_r of soil, $K_{max}=61[1+0.01(D_r-75)]$, P_a is the atmospheric pressure, $\sigma_c^{'}$ is the effective confining pressure.

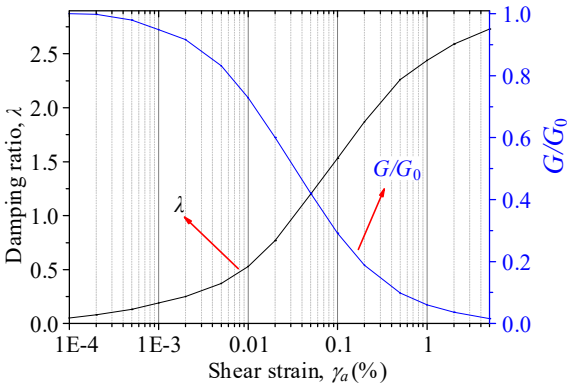

Figure 3. The curves of $G/G_{max}-\gamma_a$ and $\lambda-\gamma_a$ proposed by Seed and Idriss.

The backbone curve of soil will decline due to the development of excess pore pressure for cohesionless liquefiable soil. This shape characteristics of the backbone curve can be described according to the attenuation of *G* with the pore pressure ratio. Matasovic and Vucetic [42] established an empirical formula for the attenuation of backbone curve with the development of pore pressure ratio according to the cyclic load test results of saturated sand.

$$G_0^*=G_0(1-r_u^*)^n \quad (4)$$

where G_0^* is the maximum shear modulus at the excess pore pressure of r_u^*. n is the parameter, n ≈ 0.5 for sand.

The soil layer is divided into layers with equal heights of 0.5 m. The maximum shear modulus of soil layer under different pore pressure ratios, relative density, and confining pressure (related to soil depth) can be calculated through Eq.(2) and Eq.(3).

2.4. Lumped-Mass Model of Pile Foundation

The pile is modeled using the lumped mass model proposed by Penzien [19] in this study. Lumped mass model, which was also called multi-particle model or Mindlin static model, can simply and efficiently handle the relationship between mass, stiffness and damping in dynamic analysis [43]. The pile foundation was simplified as a series particle system, that was, the mass of the pile body was dispersed on each particle, and the particles were connected by massless beams. The pile was equally divided into several parts along the length, and the length of each part was l_e.

2.4.1. Viscosity Shear Force on Pile Section in Liquefied Soil

As shown in **Figure 4**, the viscous shear force of soil acting on the pile body is equivalently distributed in the circumference of pile-soil interface. The horizontal lateral loading of the soil acting on the pile can be expressed as:

$$\Delta P_z=4\int_0^{\frac{\pi}{2}}\frac{d}{2}\Delta L\tau_z\sin\theta d\theta \quad (5)$$

$$\Delta P_z=2\tau_z d\Delta L \quad (6)$$

Preprints (www.preprints.org) | NOT PEER-REVIEWED | Posted: 28 March 2022 doi:10.20944/preprints202110.0448.v2

Eq.(1) is substituted into Eq.(6):

$$\Delta P_z = 2\left[\eta_e + (\eta_\infty - \eta_e)(1 - r_u)\right]_z \dot{\gamma}_z d\Delta L \tag{7}$$

where ΔP_z is the lateral load of the soil on the pile body with a length of ΔL at depth of Z, d is the diameter of pile, η_∞ and η_e are the viscosity coefficient of soil when the excess pore pressure ratio r_u is equal to 0 and 1, respectively, $\dot{\gamma}_z$ is the shear strain rate of soil at depth of z. The values of η_∞ and η_e could be referred to Wang et al. [36].

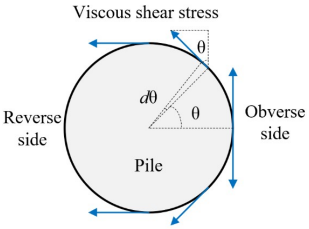

Figure 4. The force analysis of pile foundation.

2.4.2. Lateral Force on Pile in Non-Liquefiable Soil

The lateral force of the non-liquefiable soil layer acting to pile foundation is the product of soil spring coefficient (subgrade bed coefficient or reaction coefficient) and soil lateral deformation. The maximum relative horizontal displacement at different depths in the free field is applied as external boundary conditions to one end of the soil spring element which relates to the pile model. In this study, the soil spring coefficient along the depth was determined by Mindlin's solution [44–46] commonly used in the pile-soil interaction analysis. The soil spring coefficient of each node is calculated by Eq.8:

$$k_z = \frac{8\pi E_z}{3}\left\{\operatorname{arsinh}\frac{l_e - z}{r} + \operatorname{arsinh}\frac{l_e + z}{r} + \frac{2}{3r^2}\left[\frac{r^2 l_e - 2r^2 z + l_e z^2 + z^3}{\left[r^2 + (l_e + z)^2\right]^{1/2}} - \frac{z^3 - 2r^2 z}{(r^2 + z^2)^{1/2}}\right] - \right.$$
$$\left. \frac{2}{3}\left[\frac{z - l_e}{\left[r^2 + (l_e - z)^2\right]^{1/2}} - \frac{z}{(r^2 + z^2)^{1/2}}\right] + \frac{4}{3}\left[\frac{r^2 z + l_e z^2 + z^3}{\left[r^2 + (l_e + z)^2\right]^{3/2}} - \frac{r^2 z + z^3}{(r^2 + z^2)^{3/2}}\right]\right\}^{-1} \tag{8}$$

where k_z is the coefficient of soil spring at the depth of z, $E_z = 2G(1+v)$ is equivalent elastic modulus of soil at the depth of z, $r = 0.5d$ is the radius of pile, l_e is the length of pile element, which is 0.5 m in this study.

2.4.3. Horizontal Inertia Force on Pile

The inertia forces of pile were represented as static forces applied simultaneously with lateral force. The inertia forces acting on particle i along the pile in the pseudo-static method is calculated according to the following formula:

$$F_i = a_h \xi M_i \alpha_i \tag{9}$$

where F_i is the lateral inertia force of the lumped mass particle i; a_h is the lateral acceleration of the dynamic load; ξ is the reduction coefficient of seismic effect, which is 0.25; M_i is the mass of the particle i, $M_i = l_e S \rho_{pile}$; S is the sectional area of pile; α_i is dynamic distribution coefficient of inertial force of particle i, taken as 1 here; ρ_{pile} is the density of pile, which is obtained as 2400 kg/m^3.

In this study, the software ABAQUS is used to solve the quasi-static calculation problem of lumped mass model. The linear Timoshenko beam element which can reflect the shear deformation is selected in this analysis. It is assumed that the transverse shear stiffness of the beam element is linearly elastic and remains unchanged during deformation.

 doi:10.20944/preprints202110.0448.v2

3. Verification of Simplified Method

The results of centrifuge tests for pile foundation response in liquefied soil carried out by Abdoun et al. [12] and He et al. [16] are compared with the results of the simplified analysis model to verify its correctness. Moreover, the comparison of the simplified analysis method and the methods proposed by other literature are conducted to analyze the superiority of the simplified analysis method.

3.1. Cases for Verification

Abdoun et al. [12] conducted a group of centrifuge shake table tests on pile foundations in liquefaction sites. The simplified calculation model was established for Model 3 to calculate and analyze the response of pile foundation. Model 3 was composed of a 6 m overlying saturated sand layer and a 2 m underlying cemented sand layer, in which the relative density D_r and saturation density ρ of the saturated sand layer are 40% and 1961 kg/m^3. The length of the single pile is 8 m, the diameter d is 0.6 m, and the bending stiffness EI is 8000 kN·m^2. The experiment was conducted using a sine dynamic load with a frequency of 2 Hz and acceleration amplitude of 0.3 g in a prototype.

Besides, the simplified analysis method was verified and validated not only using results from the experiments but also using the data obtained from other methods. Model 1 conducted by He et al. [16] was calculated by using the simplified analysis method proposed in this study, and the bending moment and lateral deformation were compared with that obtained by other methods to validate the correctness of the simplified analysis method. Model 1 consisted of a single saturated sand layer with a thickness and relative density D_r of 5 m and 50%, respectively. A single vertical stiff pile with a length of 5 m was installed in the model, and its diameter and bending stiffness EI were 0.31 m and 14320 kN·m^2, respectively. A sine wave with a frequency of 2 Hz and the base acceleration amplitude of 0.2 g was used in this model. Details concerning two models were documented in Abdoun et al. [12] and He et al. [16,47], respectively.

3.2. Validation of Simplified Analytical Methods

3.2.1. Comparison with Results of Experiments

The comparisons between the experiment results of Abdoun et al. [12] and the simplified analysis results under different pore pressure ratios are presented in **Figure 5**. The calculated pile bending moment distribution along the depth is consistent with the test results, and the maximum bending moment occurs at the interface of sand and clay layers. The maximum bending moments at the pile bottom obtained by the test and the simplified analysis method are 122 kN·m and 139 kN·m, respectively. The error between the simplified calculation results and the test results is 14%. Furthermore, the gap between the simplified analysis results and the test results appears to increase for the bending moment measured near the soil surface. This phenomenon may be caused by the following reason: (a) the ground surface of the experimental model was inclined at a slope of 2º, which does not consider in the simplified analysis method, (b) the lateral displacement of liquefied sand is largest at the foundation surface, however, this phenomenon cannot be reflected in the one-dimensional equivalent linear analysis of the free field, which leads to a larger difference between the pile bending moment near the surface obtained from the analysis and the test. In general, the pile bending moment obtained by the simplified analysis method of pile-soil interaction considering rate-dependence is in good agreement with the results of the test. It means that the simplified analysis method of using the hydrodynamics method to analyze pile-soil interaction and viscous shear force instead of the earth pressure on pile is reasonable and feasible.

Preprints (www.preprints.org) | NOT PEER-REVIEWED | Posted: 28 March 2022 doi:10.20944/preprints202110.0448.v2

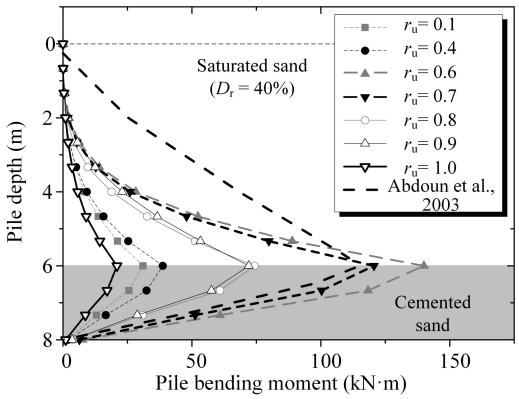

Figure 5. The comparison of computed results and test results.

Furthermore, the rate-dependent characteristic of pile-soil interaction becomes more obvious with the development of pore pressure, and the pile response increases gradually until the pile at the interbedding of sand and clay reaches a maximum bending moment of 139 kN·m at the pore water pressure ratio of 0.6. Thereafter, the pile response decreases gradually with the increase of pore pressure. When the pore water pressure ratio rises to 1.0, the maximum bending moment reduces to approximately 21 kN·m, only approximately 1/7 of the maximum value. This result shows that the seismic response of pile foundation in liquefiable soil may not reach the maximum when the soil is completely liquefied. According to the thixotropic constitutive model expressing in Eq.(1), the viscous shear stress of liquefiable soil on the pile is mainly determined by two factors: the shear strain rate of soil and the apparent viscosity representing the fluid characteristics of the soil. When the excess pore pressure ratio of soil is low, the apparent viscosity is large, nevertheless, the fluidity of foundation soil is poor, the corresponding shear strain rate is relatively small. With the increase of pore pressure, the apparent viscosity of soil decreases gradually, while the corresponding shear strain rate increases. It is noted that the development of apparent viscosity is opposite to that of the shear strain rate with the development of excess pore water pressure ratio. Therefore, the apparent viscosity and shear strain rate of soil should be comprehensively considered to evaluate the rate-dependent effect of soil on pile rather than relating to the pore pressure ratio.

It should be noted that the strongest response of the pile-soil rate-dependent interaction does not necessarily occur at the pore pressure ratio of 0.6, but possibly be related to the initial state of soil, geological conditions, soil layer distribution, dynamic load frequency, and other factors, which will be discussed in detail next.

3.2.2. Comparison with Other Methods

As shown in **Figure 6**, the response of pile obtained by the proposed method was compared with other recommendations [16] (JRA, 2020; Dobry *et al*., 2003; Gonzalez *et al*., 2005 and He *et al*., 2009).

The maximum bending moment and lateral displacement evaluated by the simplified analysis method were almost consistent with the measured peak pile response in the experiment. In comparison with the simplified analysis method, the methods recommended by JRA and Dobry et al [16]. underestimate the response of the pile, and the calculated bending moment is only about 25% of the results from centrifuge tests. As a simple approach, the simplified analysis method proposed in this study is found to predict both maximum bending moments and lateral displacements with sufficient accuracy.

Preprints (www.preprints.org) | NOT PEER-REVIEWED | Posted: 28 March 2022 doi:10.20944/preprints202110.0448.v2

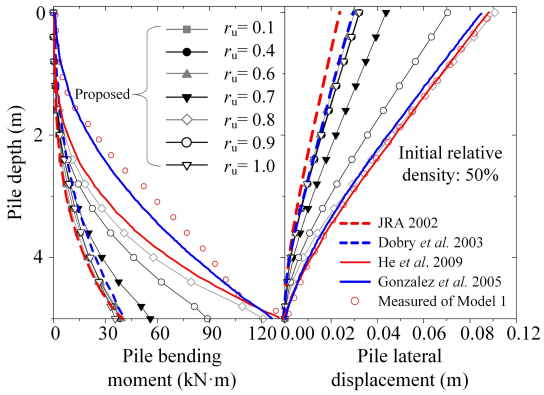

Figure 6. Comparison of pile response obtained using different method.

4. Parametric Analysis of Liquefaction Soil-Pile Interaction

Pile-soil interaction is a very complex problem, and there are many effects (such as distributional characteristics of soil, soil properties, dynamic load, pile type, etc.). The effects of relative density of soil, the thickness of non-liquefiable soil layer and dynamic loading frequency on the response of pile foundation (i.e., the bending moment and lateral displacement) are considered in this study.

4.1. Initial Relative Density of Soil

Based on Model 1 conducted by He et al. [16], three different initial relative densities of sand, which are 30%, 50%, and 70% respectively, are considered in this study to investigate the influence of the initial relative density on the pile-soil rate-dependent interaction. The distribution of bending moment and displacement of pile foundation under different initial relative densities are presented in **Figure 7**.

With the development of excess pore water pressure, the internal force and displacement response of the pile foundation can be roughly divided into two stages which are the growth stage and the attenuation stage. It is suggested that there is a threshold pore pressure that could be used to identify the stage change. When the pore pressure ratio is below the threshold pore pressure ratio, the pile response (bending moment and lateral displacement) is in the growth stage. The bending moment and lateral displacement of the pile reach the maximum values while the excess pore water pressure reached the threshold value. Once the pore pressure ratio passes this threshold, the pile response enters the fast attenuation stage.

As shown in **Figure 7**, the threshold pore pressure ratio of loose sand with the relative density of 30% is approximately 0.6, whereas the corresponding threshold pore pressure ratio for the relative density of 50% (medium dense sand) and 70% (dense sand) foundations are approximately 0.8 and 0.9, which indicating that with the increase of initial density of soil, the threshold pore water pressure ratio corresponding to the maximum pile response increases gradually. The reason is that the liquefaction resistance of the foundation soil increases with the increase of soil relative density. Therefore, a higher pore pressure ratio is required in the foundation with higher relative density to achieve the corresponding fluid characteristics, which has been confirmed in previous studies [32].

Preprints (www.preprints.org) | NOT PEER-REVIEWED | Posted: 28 March 2022 doi:10.20944/preprints202110.0448.v2

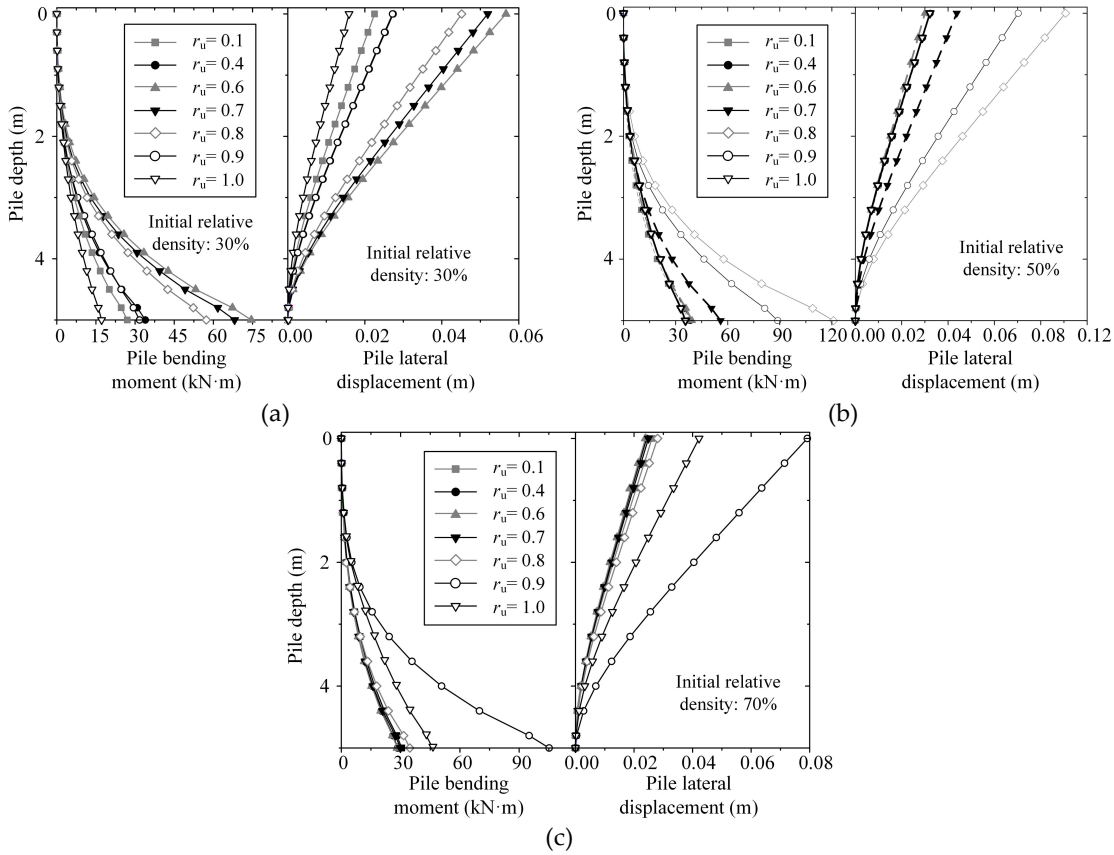

Figure 7. Effect of relative density on pile-soil interaction considering rate-dependent: (a) Relative density of 30%; (b) Relative density of 50%; (c) Relative density of 70%.

When the foundation soil is at a low pore pressure ratio level, the change of pile internal force and deformation response with the development of pore pressure ratio is not obvious, especially in the foundation with higher initial relative density. For example, in the foundation soil with a relative density of 70%, the pile bending moment distribution curve almost coincides when the pore pressure ratio increases from 0.1 to 0.7, which indicates that higher the pore pressure ratio is required to reflect the rate-dependent interaction in the foundation with higher the relative density.

The maximum bending moments of the pile under relative densities of 30%, 50%, and 70% are 75 kN·m, 124 kN·m, and 118 kN·m, respectively. Interestingly, the maximum bending moment of the pile body under the relative density of 50% case is the largest among the three cases. This result indicates that the response of pile-soil rate-dependent interaction does not monotonously develop with the initial relative density of the foundation soil. The reason may be that the apparent viscosity is smaller, and the fluidity is stronger under the same pore pressure ratio in the loose foundation, consequently, the soil with lower relative density can reach a large shear strain rate under the same shear stress. In contrast, the dense sand has a larger apparent viscosity and lower fluidity than that of the loose sand, which causes the corresponding shear strain rate to be smaller. Therefore, the apparent viscosity and shear strain rate of soil should be comprehensively considered for the effect of soil on the pile. It can be inferred that an "unfavorable" relative density is existence for the rate-dependent effect of pile-soil in some cases, which generates the greatest bending moments at the piles.

The relationship between shear strain rate and excess pore pressure ratio under the different relative densities of liquefiable sand is shown in **Figure 8**. Under the same pore pressure ratio, the denser the soil is, the smaller the shear strain rate is, which means

Preprints (www.preprints.org) | NOT PEER-REVIEWED | Posted: 28 March 2022 doi:10.20944/preprints202110.0448.v2

that the shear strain rate is inversely correlated with the relative density D_r of soil. When the excess pore pressure ratio developed to 1.0, the shear strain rate of soil with different relative densities are almost the same. The development curve of shear strain rate with pore water pressure ratio (considering D_r=50% as an example) can be divided into two stages.

- Slow development stage: The fluidity of soil increases slowly in this stage. The corresponding shear strain rate of soil with a relative density of 50% increases from 0.004 s^{-1} to 0.009 s^{-1} (increased about 2 times) while the pore pressure ratio increases from 0.1 to 0.6 (**Figure 8**). However, the increase of bending moment response of pile caused by the rate-dependent effect can be ignored (**Figure 7**(b)).
- Rapid development stage: In this stage, when the pore pressure ratio reached about 0.6, a sudden increase in the shear strain rate was observed, which means that the soil fluidity developed rapidly. The shear strain rate of the soil was considerably improved with the development of excess pore pressure, with values of 0.009 s^{-1} at r_u=0.6 and 0.13 s^{-1} at r_u=1.0. In this stage, and the pile bending moment reaches a maximum value at the excess pore pressure ratio of 0.8. For soils with different relative densities, the corresponding pore pressure ratios were different at the beginning of the rapid development stage of shear strain rate, that is, the higher the relative density, the greater the corresponding pore pressure ratio.

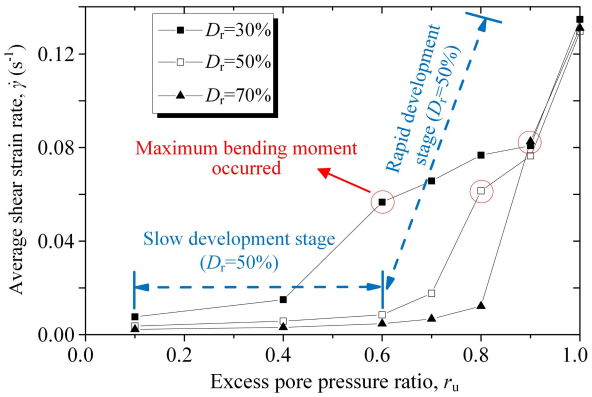

Figure 8. Variation of shear strain rate versus pore pressure ratio for different relative density.

4.2. Ratio of Non-Liquefied Layer Thickness to Liquefiable Layer Thickness

To investigate the influence of the thickness of non-liquefiable soil layer on the response of the pile, three different thickness ratios of the overlying clay layer to the liquefiable layer were considered in this study.

The distribution of the bending moment and displacement of pile under different thickness ratios H_N/H_L, which is defined as the ratio of the thickness of non-liquefiable layer in the model to that of the liquefiable layer, are presented in **Figure 9**. Comparing the bending moment curves of the pile under the three different H_N/H_L conditions, it can be found that although different thickness ratios H_N/H_L lead to a large difference bending moment of pile, the bending moment distributed curve in either condition was similar, which was distributed in an "S-shaped" along with the depth of pile, that is, there were two maxima of bending moment in the pile: i.e., one neared to the center of the sand layer and the other one located at the underlying non-liquefiable layer respectively. In addition, the maximum bending moment of the pile in the underlying non-liquefiable layer was smaller than that in the sand layer, and the trend was more obvious when the H_N/H_L decreased.

Figure 9 also shows the distribution of the displacement obtained in the analysis. The displacement distribution of the pile body along the height shows the shape of "parabola". The displacement curve of the pile has a reverse inflection point near the over-

Preprints (www.preprints.org) | NOT PEER-REVIEWED | Posted: 28 March 2022 doi:10.20944/preprints202110.0448.v2

lying clay layer due to the lateral restraint effect of the overlying clay layer on the pile. Therefore, the lateral displacement of the pile top is significantly less than those of the conditions without an overlying clay layer. Further, it was found that the lateral displacement of pile decreased with the increase of thickness of the top non-liquefiable soil layer, which was consistent with the conclusion in [48].

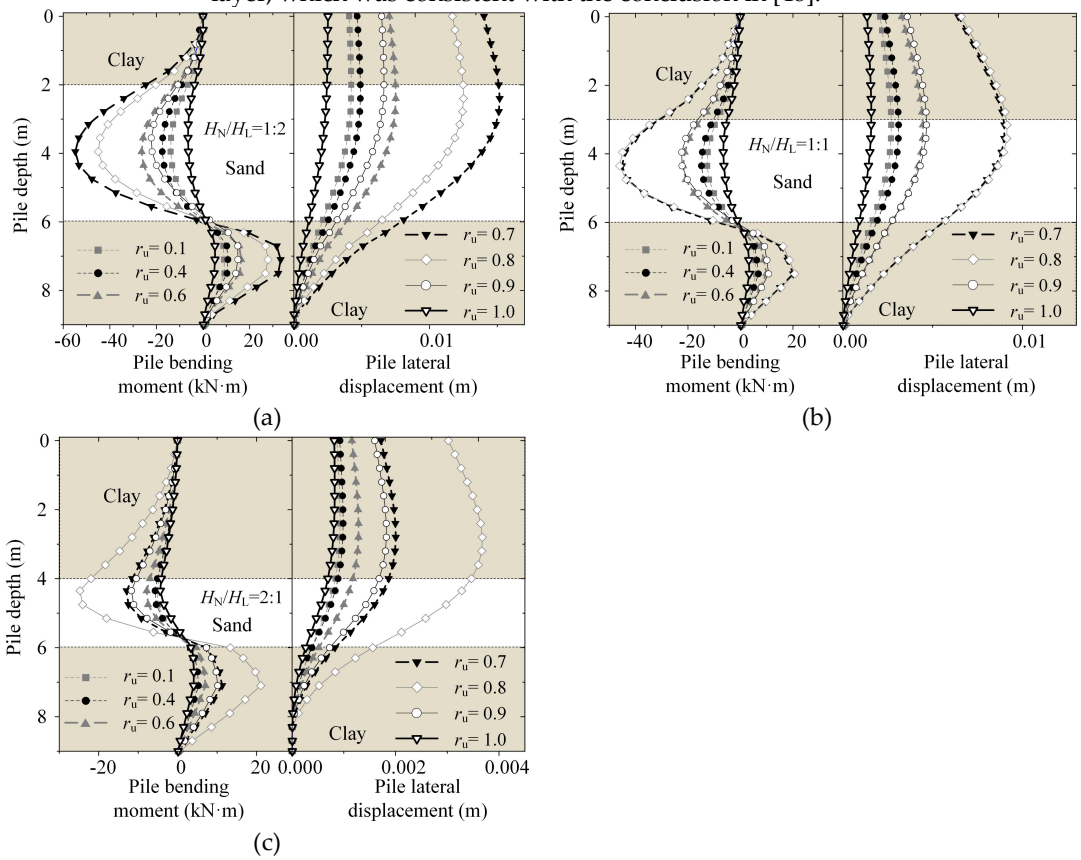

Figure 9. The bending moment and lateral displacement of pile under the foundations with different H_N/H_L: (a) H_N/H_L=1:2; (b) H_N/H_L=1:1; (c) H_N/H_L=2:1.

When H_N/H_L is 1:2, the maximum bending moment of the pile appears in the middle of the sandy soil layer, and the maximum lateral displacement of the pile appears around the boundary between the sandy soil layer and the overlying clay layer. With the increase of H_N/H_L, the maximum bending moment of the pile gradually decreases, and its position gradually moves upward from the liquefiable layer to the boundary between the overlying non-liquefiable layer and the liquefiable layer. The corresponding inflection point of the lateral displacement curve gradually moves from the sandy soil layer to the overlying clay layer, which is caused by the different fluidity of the liquefiable layer under different thickness ratios.

It is obvious that with the increase of H_N/H_L, not only the maximum bending moment of pile foundation decreases but also the threshold excess pore pressure ratio corresponding to the maximum bending moment is higher, indicating that when the liquefied soil layer is thin or deeply buried, the conditions required for the soil to reflect its flow characteristics are relatively harsh. Therefore, the pile-soil rate-dependent interaction is inapparent.

4.3. Frequency of Dynamic Load

The frequency of dynamic load has a great influence on the foundation soil response and soil-structure interaction. Six different frequencies were considered in this study to

 doi:10.20944/preprints202110.0448.v2

reveal the effect of the frequency of dynamic load on the pile-soil rate-dependent interaction.

The distributions of pile bending moment along with the depth under different dynamic frequency *f* are compared in **Figure 10**. The pile-soil rate-dependent interaction is significantly correlated with the frequency of input ground motion. The inputted ground motion frequency corresponding to the bending moment of pile reached its peak value gradually transformed from 4 Hz to 1 Hz with the soil pore pressure ratio developed from 0.1 to 1.0 (As shown in **Figure 10** and **Table 1**). The reason for the above phenomenon is that the natural frequency of soil gradually decreases as a result of the loss of stiffness and strength associated with the excess pore water pressure generation, and the field is increasingly sensitive to long-period dynamic loads.

For the field with an initial relative density of 30%, when the input dynamic load period is relatively long (i.e., 1Hz and 2Hz), the bending moment response of pile could be divided into growth stage and attenuation stage with the development of pore pressure, i.e., there was a threshold pore pressure ratio. In contrast, the pile bending moment response decreased gradually with the development of pore water pressure when the dynamic frequency was relatively high (i.e., 3Hz, 4Hz, 5Hz and 6Hz in this study), which indicated that the threshold did not exist in those cases. It could be because, with the development of pore pressure, the fluidity was increased, however, the filter effect of softened soil on the high-frequency ground motion was also obvious. Therefore, the pile foundation response under high-frequency load decreased monotonically with the development of pore pressure. Moreover, when the excess pore pressure ratio of soil was high, the bending moment response of pile under high-frequency load is smaller than that under low-frequency load.

By comparing the pile bending moment of different cases (**Table 1**), it should be noted that the smaller the input ground motion frequency, the higher the threshold pore pressure ratio, and the smaller the pile bending moment corresponding to the threshold pore pressure ratio. This observation indicated that whether there is a threshold pore water pressure ratio, and its value is related to relative density, soil layer distribution, dynamic load frequency, etc.

The significance of the above observations may be better understood by reference to the relationship between the shear strain rate of soil and the excess pore pressure ratio in different loading frequencies, shown in **Figure 11**. With the excess pore pressure developed from 0.1 to 1.0, the vibration frequency of the case corresponding to the maximum shear strain rate of soil decreases from 4 Hz to 1 Hz, which was primarily a result of the decrease of soil natural frequency caused by the increase of excess pore pressure. Furthermore, the shear strain rate of soil increased in all conditions when the pore water pressure ratio reaches 1.0 as shown in **Figure 11**. However, the increased amplitude of shear strain rate under the conditions with the higher frequency load (3Hz, 4Hz, 5Hz and 6Hz) were less than that under the conditions with lower input frequencies (1 Hz and 2 Hz). This is because that the soil stiffness decreased due to the development of excess pore pressure ratio, result in the high-frequency motions cannot be traveled to the upper soil (the filtering effect of liquefied soil on high-frequency load), therefore the shear strain rate was relatively smaller for the cases that the model was subjected to higher frequency.

Preprints (www.preprints.org) | NOT PEER-REVIEWED | Posted: 28 March 2022 doi:10.20944/preprints202110.0448.v2

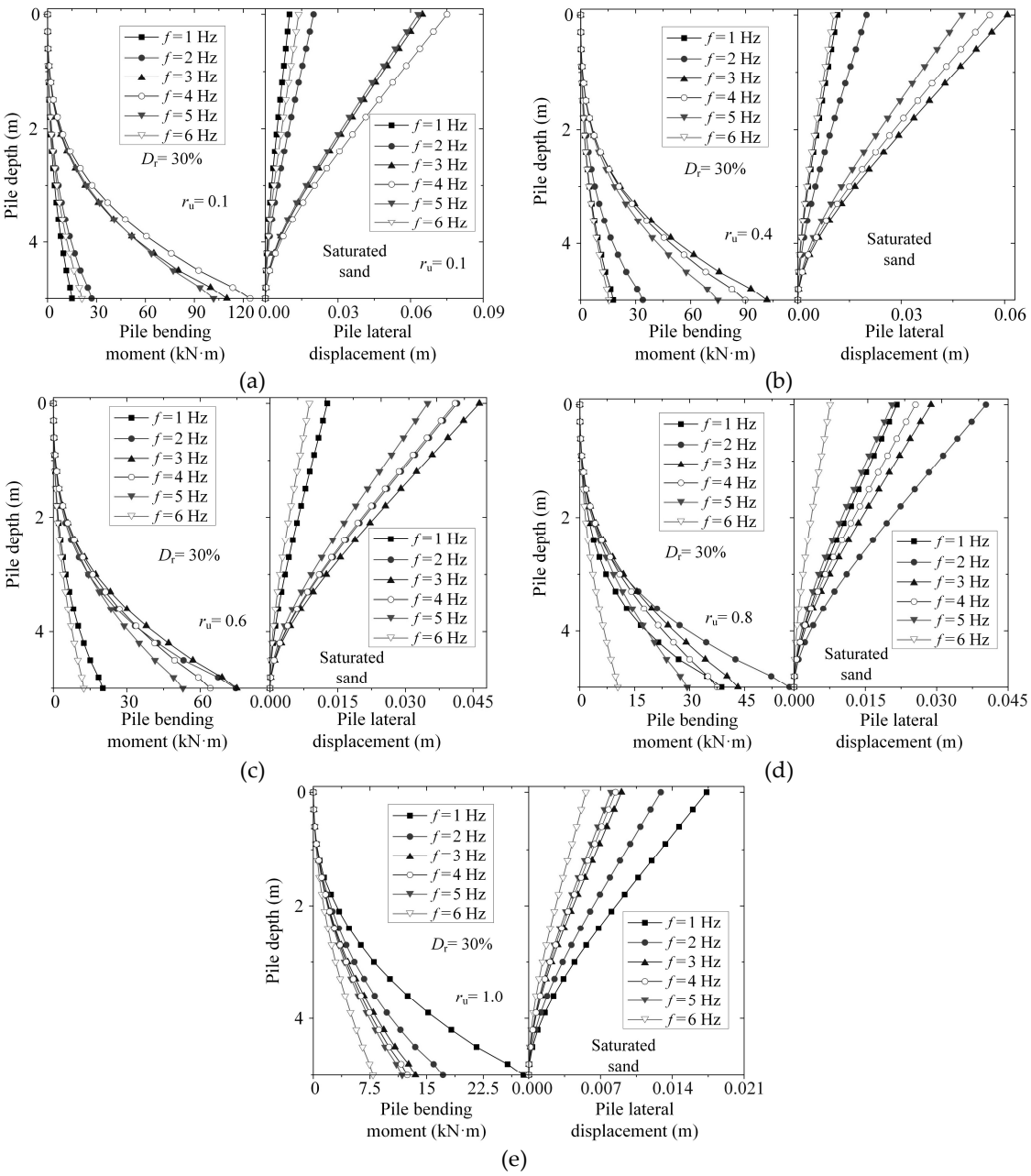

Figure 10. Bending moment and lateral displacement of pile under different loading *f*: (a) $r_u = 0.1$; (b) $r_u = 0.4$; (c) $r_u = 0.6$; (d) $r_u = 0.8$; (e) $r_u = 1.0$.

Table 1. The bending moment of pile in different loading frequency (kN·m).

f (Hz)	Bending moment (kN·m)				
	$r_u = 0.1$	$r_u = 0.4$	$r_u = 0.6$	$r_u = 0.8$	$r_u = 1.0$
1	14.9	17.9	20.3	38.7	27.8
2	27	33.9	74.6	57.3	17.1
3	110	101.7	75	43.2	13.5
4	124.2	89.7	64.2	37.5	12.5
5	101.7	75	53	29.4	11.7
6	21.2	15.5	12.5	10.4	8

Preprints (www.preprints.org) | NOT PEER-REVIEWED | Posted: 28 March 2022 doi:10.20944/preprints202110.0448.v2

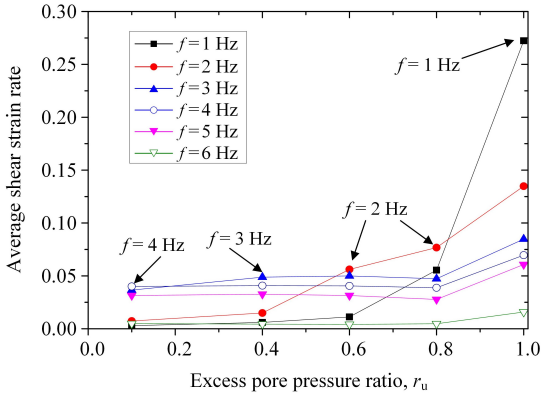

Figure 11. Shear strain rate versus pore pressure ratio for different loading frequency.

5. Conclusions

In this study, a simplified analysis method, which considering the rate-dependent effect of the liquefied sand on the pile and models the liquefied sand with a thixotropic fluid, was proposed to evaluate the behavior of free-head single pile embedded in homogenous and layered liquefiable soil. The calculation results were compared with that of Abdoun's tests to verify the validity of the proposed simplified analysis method. Then, the effects of relative density, pore pressure ratio, the thickness of overlying clay layer, and dynamic load frequency on the rate-dependent characteristic of pile-soil were discussed. The main conclusions can be drawn as follows:

(1) The simplified analysis method based on the hydrodynamics method, which adopting viscous shear force (related to the shear strain rate and apparent viscosity of soil) instead of the soil pressure on the pile to analyze pile-soil interaction, is practical. The distribution of bending moment along height obtained by the simplified method in this study is good agreement with that of tests, and the maximum bending moment occurred near to the interface of liquefiable-nonliquefiable soil layer.

(2) The pile bending moment and displacement response do not necessarily change monotonically with the development of the excess pore pressure ratio. There exists a threshold pore water pressure ratio (i.e., when D_r is 30%, 50% and 70%, threshold pore pressure ratio r_u is 0.6, 0.8 and 0.9, respectively), resulting in the pile bending moment and displacement greater than those of other pore water pressure ratios. Based on the threshold pore water pressure ratio, the response of the pile can be divided into two stages, that is, the growth stage and the attenuation stage.

(3) The maximum bending moment of the pile under the relative density of 50% case is larger than that under the other two relative densities. An “unfavorable” relative density, which maximizes the pile response under the same other conditions (excess pore pressure ratio, dynamic load), is existence for the pile-soil interaction effect.

(4) Whether there is the threshold pore water pressure ratio, and its value is related to the relative density of soil, the thickness of overlying clay layer, and the vibration frequency. Compared with the higher frequency load conditions, the threshold pore pressure ratio is more prone to occur in the conditions with relatively lower frequency. Furthermore, the higher the relative density, the thicker the overlying clay layer, and the greater the threshold pore water pressure ratio. When the soil is in the state of high pore pressure ratio, the pile foundation response under high-frequency dynamic load is less than that under low-frequency dynamic load, which is caused by the high-frequency filtering effect of soil under low effective stress.

Author Contributions: Conceptualization, X.Z. and Z.W.; methodology, X.Z. and H.G.; software, X.Z.; validation, H.G. and Z.W.; formal analysis, W.L.; investigation, H.G. and W.L.; resources,

Z.W.; data curation, Z.J.; writing—original draft preparation, X.Z. and Z.J.; writing—review and editing, Z.J.; visualization, Z.J.; supervision, X.Z. All authors have read and agreed to the published version of the manuscript.

Funding: This research was funded by the National Natural Science Foundation of China (No. 52178336, No. 52108324 and No. 52108298), the Natural Science Research Project of Colleges and Universities in Jiangsu Province of China (No. 18KJA560002) and the Middle-Aged and Young Science Leaders of Qinglan Project of Universities in Jiangsu Province of China.

Institutional Review Board Statement: Not applicable.

Informed Consent Statement: Not applicable.

Data Availability Statement: The data are contained within the article.

Conflicts of Interest: The authors declare no conflict of interest.

References

1. Rajeswari, J.S.; Sarkar, R. Seismic behavior of batter pile groups embedded in liquefiable soil. *Earthq Eng Eng Vib*. 2021, 20, 583–604. https://doi.org/10.1007/s11803-021-2040-9.
2. Mohanty, P.; Xu, D.; Biswal, S.; Bhattacharya, S. A shake table investigation of dynamic behavior of pile supported bridges in liquefiable soil deposits. *Earthq Eng Eng Vib*. 2021, 20, 1–24. https://doi.org/10.1007/s11803-021-2002-2.
3. Zhou, G.; Chen, Y; Liu, H. Preliminary study on flow constitutive model of post liquefied sand in zero effective stress state. *Int. Efforts Lifeline Earthq. Eng.* 2013, 632–639. https://doi.org/10.1061/9780784413234.081.
4. Hochi, Y.; Murono, Y.; Saitoh, M.; Goit, C.S. Earthquake motion filtering effect by pile foundations considering nonlinearity of soil and piles. *Soil Dyn Earthq Eng.* 2019, 125, 105748. https://doi.org/10.1016/j.soildyn.2019.105748.
5. Li, W.; Chen, Y.; Stuedlein, A.W.; Liu, H.; Zhang, X.; Yang, Y. Performance of X-shaped and circular pile-improved ground subject to liquefaction-induced lateral spreading. *Soil Dyn Earthq Eng*. 2018, 109, 273–281. https://doi.org/10.1016/j.soildyn.2018.03.022.
6. Ebeido, A.; Elgamal, A.; Tokimatsu, K.; Abe, A. Pile and pile-group response to liquefaction-induced lateral spreading in four large-scale shake-table experiments. *J Geotech Geoenviron.* 2019, 145, 04019080. https://doi.org/10.1061/(asce)gt.1943-5606.0002142.
7. Qu, L.; Ding, X.; Kouroussis, G.; Zheng, C. Dynamic interaction of soil and end-bearing piles in sloping ground: Numerical simulation and analytical solution. *Comput Geotech*. 2021, 134, 1–16. https://doi.org/10.1016/j.compgeo.2020.103917.
8. Dobry, R.; Abdoun, T.; O'Rourke, T.D.; Goh, S.H. Single piles in lateral spreads: Field bending moment evaluation. *J Geotech Geoenviron.* 2003, 129, 879–89.
9. Wilson, D.W.; Boulanger, R.W.; Kutter, B.L. Observed seismic lateral resistance of liquefying sand. *J Geotech Geoenviron*. 2000, 126, 898–906. https://doi.org/10.1061/(asce)1090-0241(2000)126:10(898).
10. Wu, Q.; Ding, X.; Zhang, Y.; Chen, Z. Comparative study on seismic response of pile group foundation in coral sand and Fujian sand. *J Mar Sci Eng*. 2020, 8, 189. https://doi.org/10.3390/jmse8030189.
11. Rollins, K.M.; Gerber, T.M.; Lane, J.D.; Ashford, S.A. Lateral resistance of a full-scale pile group in liquefied sand. *J Geotech Geoenviron.* 2005, 131, 115–125. https://doi.org/10.1061/(ASCE)1090-0241(2005)131:1(115).
12. Abdoun, T.; Dobry, R.; O'Rourke, T.D.; Goh, S.H. Pile response to lateral spreads: Centrifuge modeling. *J Geotech Geoenviron.* 2003, 129, 869–878. https://doi.org/10.1061/(ASCE)1090-0241(2003)129:10(869).
13. Towhata, I.; Thi, T.; Anh, L.; Yamada, S.; Motamed, R.; Kobayashi, Y. Zero-gravity triaxial shear tests on mechanical properties of liquefied sand and performance assessment of mitigations against large ground deformation. *5th Int. Conf. Recent Adv. Geotech. Earthq. Eng. soil Dyn.* 2010, 24–29. https://scholarsmine.mst.edu/icrageesd/05icrageesd/session12/11.
14. Knappett, J.A.; Madabhushi, S.P.G. Influence of axial load on lateral pile response in liquefiable soils. Part II: numerical modelling. *Géotechnique*, 2009, 59, 583–592. https://doi.org/10.1680/geot.8.010.3750.

 doi:10.20944/preprints202110.0448.v2

15. Lu, C.W.; Chang, D.W. Case study of dynamic responses of a single pile foundation installed in coal ash landfills using effective stress analysis and EQWEAP. *Geotech Eng*, 2015, 46, 77–81.
16. He, L.; Elgamal, A.; Abdoun, T.; Abe, A.; Dobry, R.; Hamada, M.; Menses, J.; Sato, M.; Shantz, T.; Tokimatsu, K. Liquefaction-induced lateral load on pile in a medium D_r sand layer. *J Earthq Eng*. 2009, 13, 916–938. https://doi.org/10.1080/13632460903038607.
17. Kavitha, P.E.; Beena, K.S.; Narayanan, K.P. A review on soil – structure interaction analysis of laterally loaded piles. *Innov Infrastruct So.* 2016, 1, 1–15. https://doi.org/10.1007/s41062-016-0015-x.
18. Dash, S.R.; Bhattacharya, S.; Blakeborough, A.; Hyodo, M. P-Y curve to model lateral response of pile foundations in liquefied soils. *14th World Conf Earthq Eng.* 2008, 14, 1–8.
19. Penzien, J.; Scheffey, C.F.; Parmelee, R.A. Seismic analysis of bridges on long piles. *J Eng Mech Div*. 1964, 90, 223–254. https://doi.org/10.1061/JMCEA3.0000489.
20. Novak, M. Dynamic stiffness and damping of piles. *Can Geotech J*. 1974, 11, 574–598. https://doi.org/10.1139/t74-059.
21. Nogami, T.; Konagai, K. Time domain axial response of dynamically loaded single piles. *J Eng Mech.* 1986, 112, 1241–1252. https://doi.org/10.1061/(ASCE)0733-9399(1986)112:11(1241).
22. Naggar, M.E.; Novak, M. Non-linear model for dynamic axial pile response. *J Geotech Eng*. 1994, 120, 308–329. https://doi.org/10.1061/(ASCE)0733-9410(1994)120:2(308).
23. Boulanger, R.W.; Curras, C.J.; Kutter, B.L.; Wilson, D.W.; Abghari, A. Seismic soil-pile-structure interaction experiments and analyses. *J Geotech Geoenviron.* 1999, 125, 750–759. https://doi.org/10.1061/(ASCE)1090-0241(1999)125:9(750).
24 Goh, S. Limit state model for soil-pile interaction during lateral spread. *In Proc. 7th. US-Japan Workshop on Earthquake Resistant Design of Lifeline Facilities and Countermeasures against Soil Liquefaction*, Seattle, WA, 1999.
25 Bhattacharya S, Bolton M D, Madabhushi S P G. A reconsideration of the safety of piled bridge foundations in liquefiable soils. *Soils and foundations*. 2005, 45(4): 13-25.
26 Liu, L and Dobry, R. Effect of liquefaction on lateral response of piles by centrifuge model tests. *NCEER Bulletin.* 1995, 9(1): 7-11. https://rosap.ntl.bts.gov/view/dot/13895.
27. Lombardi, D.; Dash, S.R.; Bhattacharya, S.; Ibraim, E.; Muirwood, D.; Taylor, C.A. Construction of simplified design p–y curves for liquefied soils. *Géotechnique.* 2017, 67, 216–227. https://doi.org/10.1680/jgeot.15.P.116.
28. Takahashi, H.Ã.; Takahashi, N.; Morikawa, Y.Ã.; Towhata, I.; Takano, D.Ã. Efficacy of pile-type improvement against lateral flow of liquefied ground. *Géotechnique.* 2016, 66, 617–626. https://doi.org/10.1680/jgeot.14.P.238.
29. Chen, Y.; Liu, H.; Wu, H. Laboratory study on flow characteristics of liquefied and post-liquefied sand. *Eur J Environ Civ Eng.* 2013, 17, 23–32. https://doi.org/10.1080119648189.2013.834583.
30. Chen, Y.; Wu, H.; Sha, X.; Liu, H. Laboratory tests on flow characteristics of pre-liquefied sand. *Int. Efforts Lifeline Earthq. Eng.* 2013, 600–607. https://doi.org/10.1061/9780784413234.077.
31. Chen, Y.; Xu, C.; Liu, H.; Zhang, W. Physical modeling of lateral spreading induced by inclined sandy foundation in the state of zero effective stress. *Soil Dyn Earthq Eng*. 2015, 76, 80–85.
32. Ye, B.; Ni, X.; Huang, Y.; Zhang, F. Unified modeling of soil behaviors before/after flow liquefaction. *Comput Geotech*. 2018, 102, 125–135. https://doi.org/10.1016/j.compgeo.2018.06.011.
33. Hwang, J.I.; Kim, C.Y.; Chung, C.K.; Kim, M.M. Viscous fluid characteristics of liquefied soils and behavior of piles subjected to flow of liquefied soils. *Soil Dyn Earthq Eng*. 2006, 26. 313–323. https://doi.org/10.1016/j.soildyn.2005.02.020.
34. Marinelli, F.; Pisanó, F.; Prisco, C.D.; Buscarnera, G. Model-based interpretation of undrained creep instability in loose sands. *Géotechnique*. 2018, 68, 504–517. https://doi.org/10.1680/jgeot.16.P.257.
35. Towhata, I.; Anh, T.T.L.; Motamed, R.; Sesov, V. Rate dependent nature of liquefied sand undergoing large flow deformation and its interaction with group pile foundation. *Proc. Int. Offshore Polar Eng. Conf.* 2009, 1, 1–8.

36. Wang, Z.; Ma, J.; Gao, H.; Stuedlein, A.W.; He, J.; Wang, B. Unified thixotropic fluid model for soil liquefaction. *Géotechnique.* 2020, 70, 849–862. https://doi.org/10.1680/jgeot.17.P.300.
37. Mao, W.; Liu, B.; Rasouli, R.; Aoyama, S.; Towhata, I. Performance of piles with different configurations subjected to slope deformation induced by seismic liquefaction. *Eng Geol*. 2019, 263, 105355. https://doi.org/10.1016/j.enggeo.2019.105355.
38 Mindlin R D. Force at a point in the interior of a semi-infinite solid. *Physics*. 1936, 7(5): 195-202.
39 Guoxing C, Enquan Z, Zhihua W, et al. Experimental investigation on fluid characteristics of medium dense saturated fine sand in pre-and post-liquefaction. *Bulletin of Earthquake Engineering*. 2016, 14(8): 2185-2212.
40. Seed, H.B.; Idriss, I.M. Soil moduli and damping factors for dynamic response analysis. California; Berkely: 1970.
41. Seed, H.B.; Wong, R.T.; Idriss, I.M.; Tokimatsu, K. Moduli and damping factors for dynamic analyses of cohesionless soils. *J Geotech Eng.* 1986, 112, 1016–1032. https://doi.org/10.1061/(ASCE)0733-9410(1986)112:11(1016).
42. Matasović, N.; Vucetic, M. Cyclic characterization of liquefiable sands. *J Geotech Eng*. 1993, 119, 1805–1822. https://doi.org/10.1061/(ASCE)0733-9410(1993)119:11(1805).
43. Ruan, H.; He, Y.; Wang, W. Research on pile-soil-structure dynamic interaction of large span cable-stayed bridge by using lumped mass model. *Hans J Civ Eng*. 2018, 7, 596–605. https://doi.org/10.12677/HJCE.2018.74069.
44. Penzien, J. *Soil-pile foundation interaction. Earthq. Eng.* Englewood Cliffs: Scopus, USA, 1970; p. 349–381.
45. Douglas, D.J.; Davis, E.H. The movement of buried footings due to moment and horizontal load and the movement of anchor plates. *Géotechnique.* 1964, 14, 115–132. https://doi.org/10.1680/geot.1964.14.2.115.
46. Liyanapathirana, D.S.; Poulos, H.G. Seismic lateral response of piles in liquefying soil. *J Geotech Geoenviron*. 2005, 131, 1466–1479. https://doi.org/10.1061/(asce)1090-0241(2005)131:12(1466).
47. Liang, C.H. *Liquefaction-induced lateral spreading and its effects on pile foundations*. University of California: San Diego, USA, 2005.
48. Fiky, N.E.E.; Metwally, K.G; Akl, A.Y. Effect of top soil liquefaction potential on the seismic response of the embedded piles. *Ain Shams Eng J*. 2020, 11, 923–931. https://doi.org/10.1016/j.asej.2020.03.002.